

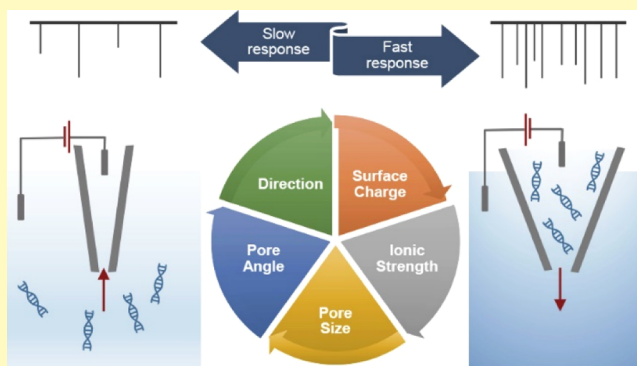
Quantitative Analysis of Factors Affecting the Event Rate in Glass Nanopore Sensors

Reza Nouri,[†] Zifan Tang,[†] and Weihua Guan^{*,†,‡,§}[†]Department of Electrical Engineering and [‡]Department of Biomedical Engineering, Pennsylvania State University, University Park, Pennsylvania 16802, United States

Supporting Information

ABSTRACT: While the solid-state nanopore sensors have shown exceptional promise with their single-molecule sensitivity and label-free operations, one of the most significant challenges in the nanopore sensor is the limited analyte translocation event rate that leads to prolonged sensor response time. This issue is more pronounced when the analyte concentration is below the nanomolar (nM) range, owing to the diffusion-limited mass transport. In this work, we systematically studied the experimental factors beyond the intrinsic analyte concentration and electrophoretic mobility that affect the event rate in glass nanopore sensors. We developed a quantitative model to capture the impact of nanopore surface charge density, ionic strength, nanopore geometry, and translocation direction on the event rate. The synergistic effects of these factors on the event rates were investigated with the aim to find the optimized experimental conditions for operating the glass nanopore sensor from the response time standpoint. The findings in the study would provide useful and practical insight to enhance the device response time and achieve a lower detection limit for various glass nanopore-sensing experiments.

KEYWORDS: nanopore, electroosmotic flow, modeling, event rate, response time



Solid-state nanopores made with silicon nitride,^{1–3} glass,^{4–6} and graphene,⁷ have become a versatile single-molecule analytical tool for label-free analysis of individual nucleic acids and protein molecules.^{8–11} The nanopore sensor is usually operated by applying a small voltage bias across the nanometer-sized pore separating two chambers filled with electrolyte, and the resulting ionic current through the pore (~0.01–100 nA) represents the readout signal.^{12,13} As the charged biomolecule is electrophoretically driven through the nanopore, the transient change in the ionic current indicates the passage of an analyte (often called an event). The shape, duration, magnitude, and frequency of these translocation events provide information about the molecule of interest (e.g., size,¹⁴ charge,² and concentration¹⁵). Although the nanopore sensor itself has single-molecule sensitivity and resolution, a significant challenge in nanopore sensing is the prolonged sensor response time when analyte concentration decreases.¹⁶ This issue stems from the diffusion-limited mass transport in nanopore sensors, resulting in the lack of efficiency for sampling sufficient numbers of molecules from the analyte solution.¹⁷ Freedman et al. estimated that if the solution concentration is sub-picomolar, then there would only be 0.03 molecules in the capture volume, requiring more than 1 h measurement time to observe a single event.¹⁸ In our previous study of using a glass nanopore as a digital single-molecule counter, we have shown that the relative uncertainty (δ) of

inferring the event rate is $n^{-1/2}$, where n is the number of events. From the practical perspective, if one can only tolerate a maximal uncertainty percentage of δ_{\max} and a maximal experimental time T_{\max} , then a minimal event rate of $1/(\delta_{\max}^2 T_{\max})$ would be necessary (Figure S1). As a result, the event rate is of significant importance for achieving quicker sensor response and lower detection limits.^{19–21}

While molecular transport through nanopores has been studied previously by examining the effect of applied voltage,^{14,22} temperature, salt concentration,²³ translocation direction,²³ and the surface charge,²⁴ only a few works were dedicated to addressing the event rate issue. For instance, to increase the flux of DNA to the nanopore, Wanunu et al.¹⁴ applied asymmetric electrolyte solutions on both sides of the nanopore to increase the electric field, focusing more molecules into the pore. Freedman et al.¹⁸ employed single-molecule dielectrophoretic trapping to overcome the diffusion-limited motion of DNA toward the nanopore. In another study, localized optical heating of the plasmonic nanostructures at the nanopore was used to precisely control the temperature near the nanopore,²⁵ which could be used to enhance the DNA event rate.²⁶ Most of these studies used external apparatus and

Received: August 10, 2019

Accepted: October 15, 2019

Published: October 15, 2019

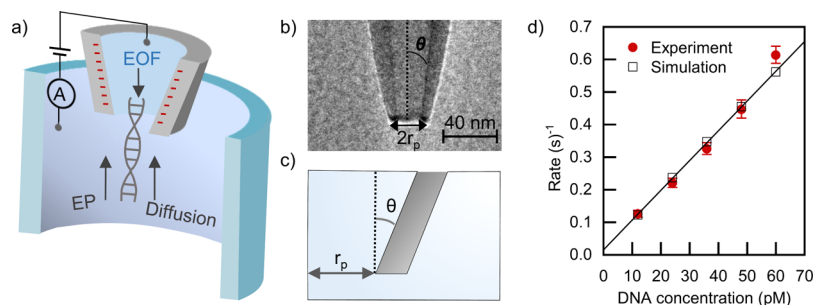


Figure 1. (a) Interplay between diffusion, electrophoresis, and EOF determines the molecule transportation through nanopores. (b) Transmission electron microscopy image of a typical conical-shaped glass nanopore. (c) Schematic view of the nanopipette tip in the computational domain. The nanopipette geometry was defined by its diameter ($2r_p$) and angle (θ). (d) Validation of the model by comparing the simulation and experiment results, using 5 kb DNA at 1 M KCl under 400 mV bias. The diameter of the nanopore is 12 nm.

components to enhance the translation rate. It remains less explored how the intrinsic nanopore properties and experimental configurations (surface charge, geometry, salt concentration, and translocation direction) affect the event rate in a synergistic study.

In this work, we performed a quantitative study on the effect of these experiment-relevant parameters on the event rates in the glass nanopore sensors. We developed a numerical model to evaluate the DNA event rate through the glass nanopore, which was validated by the experimental results. We systematically elucidated the effect of nanopore surface charge and ionic strength on the event rate of DNA through the conical shape nanopores. We examined the impact of various nanopore geometries (asymmetric nanopipette-based and symmetric membrane-based) on the event rate and their sensitivity to the change of surface charge and ionic strength. The event rate was found to be highly dependent on the direction of translation for asymmetric nanopores. We anticipate that this event rate-focused study would provide useful and practical insight to enhance the device response time and achieve a lower detection limit for various glass nanopore-sensing experiments.

MATHEMATICAL MODEL

Conceptually, the nanopore event rate is controlled by the slowest processes in the following three steps: (1) the DNA moves from the bulk toward the pore entrance by a combination of diffusion and drift forces; (2) the DNA is captured at the entrance of the nanopore; and (3) the DNA overcomes an entropy energy barrier and goes through the nanopore, causing a detectable ionic current blockade. Depending on the experimental conditions, the voltage-driven translocation of DNA molecules can be diffusion-limited or barrier-limited.²² Because most of the glass nanopores used in the experiments were with size at least 10 nm in diameter, and the voltage applied is less than 500 mV, the diffusion-limited mechanism is dominant in most of the glass nanopore experiments (Supporting Information Note S1). As a result, our model will focus on the diffusion-limited regime without considering the nanopore–molecular interactions.

In the diffusion-limited regime, the molecular translocation through the nanopore is determined by the interplay between three motions: diffusion, electrophoresis (EP), and electroosmotic flow (EOF, Figure 1a). The event rate is the outcome of these three forces. The Poisson–Nernst–Planck (eqs 1 and 2), Navier–Stokes and continuity (eqs 3 and 4) equations were used to capture the electric field, ionic and molecule

concentration, and electroosmotic velocity distribution as follows

$$\nabla^2 V = -\rho_e / \epsilon_0 \epsilon_r \quad (1)$$

$$\nabla \cdot J_i = 0 \quad (2)$$

$$\nu \nabla^2 u - \nabla p - \rho_e \nabla V = 0 \quad (3)$$

$$\nabla \cdot u = 0 \quad (4)$$

in which V is the electric potential; $\rho_e = eN_A(\sum_i z_i c_i)$ is the charge density of mobile ions. ϵ_0 and ϵ_r is the vacuum and relative permittivity, respectively. Note that the DNA charge density was not taken into consideration for calculating the potential distribution because their concentration (\sim pM to nM) is negligible as compared to that of ions (\sim mM). In addition, the intermolecular interaction was not taken into consideration because the average distance between molecules will be a few micrometers when the concentration is less than 100 pM (Supporting Information Note S2). The molecular and ionic flux density J_i is given by

$$J_i = -D_i \nabla c_i + c_i (u - z_i \mu_i \nabla V) \quad (5)$$

where D_i , μ_i , z_i , and c_i are the diffusivity, mobility, valance, and concentration of each species. In Navier–Stokes and continuity equations (eqs 3 and 4), u , p , and ν are velocity, pressure, and viscosity of the fluid, respectively. The molecular event rate R (s^{-1}) was obtained by integrating the molecules flux over the pore entrance area as

$$R = N_A \int_S J_{\text{molecules}} dS \quad (6)$$

where S is the surface area spanning the cross-section of the pore entrance.

The strongly coupled mathematical model was numerically solved with COMSOL Multiphysics. A two-dimensional axisymmetric computational domain was used to study the effect of surface charge, ionic strength, and nanopore geometry on the event rate (see Figure S2 and Table S1 for details). The nanopore geometry was modeled after a typical conical-shaped glass nanopore (Figure 1b) by its radius r_p and angle θ (Figure 1c). The reservoir and glass nanopore were assumed to be large enough such that the ionic concentration far away from the pore is the bulk value. A voltage bias is applied between the two electrodes positioned far away from the pore.

In order to validate the model, we computed the event rate of 5 kb DNA at five different concentrations through a glass

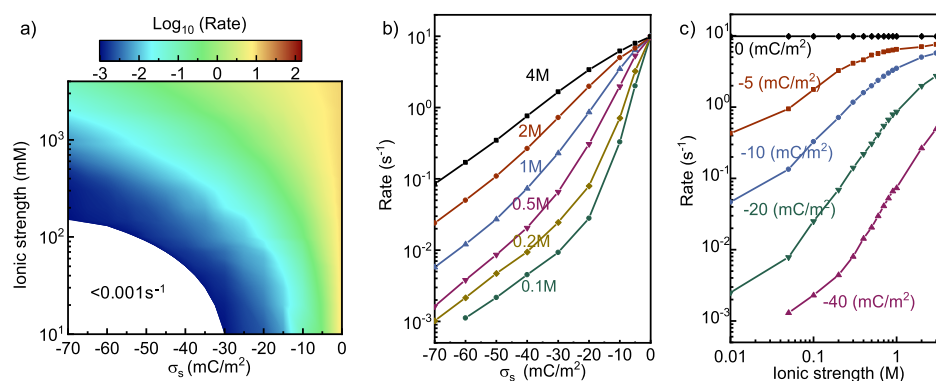


Figure 2. (a) Event rate of 100 pM DNA through a conical-shaped nanopore (12 nm diameter) for a different range of ionic strength (10 mM to 4 M) and surface charge density (0 to -70 mC/m²). (b) Effect of surface charge density on the event rate at various ionic strengths. (c) Effect of ionic strength on the event rate at various surface charge densities.

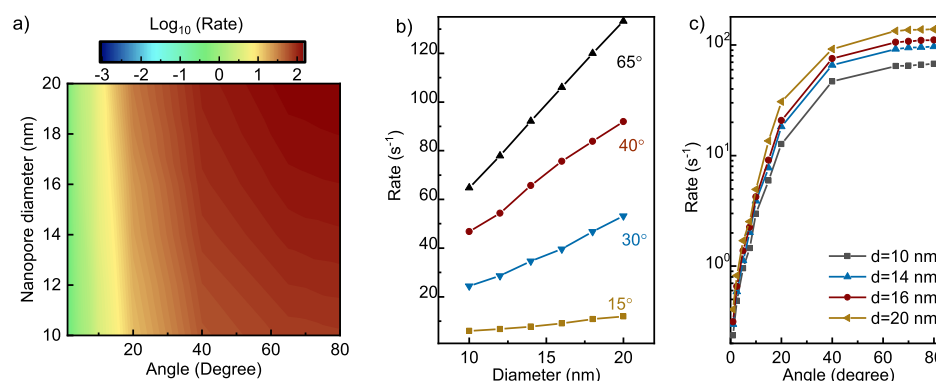


Figure 3. (a) Event rate for 100 pM DNA through the nanopore at an ionic strength of 1 M and surface charge density of -20 mC/m² with different diameters and angles. (b) Effect of nanopore diameter on the event rate at different angles. (c) Effect of nanopore angle on the event rate at different sizes.

nanopore ($r_p = 6$ nm and $\theta = 4^\circ$) at 1 M KCl under 400 mV bias voltage. The numerical results were benchmarked to our previous experimental study.¹⁵ In the simulation, we assumed the nanopore wall surface charge density of -20 mC/m² and the DNA mobility of 8×10^{-8} m²/V s, which is close to these derived from the experimental measurement.^{27,28} As shown in Figure 1d, an excellent agreement between the experimental and simulation results was obtained, confirming the validity of the mathematical model for evaluating the event rate. Note that the molecule electrophoretic mobility could also affect the event rate. Our numerical results (Figure S3) as well as previous analytical results²² show that the event rate is linearly dependent on the molecular mobility in the diffusion-limited regime. In this work, we aim to study the factors affecting the event rates beyond the intrinsic analyte concentration and electrophoretic mobility.

RESULTS AND DISCUSSION

Impact of Surface Charge and Ionic Strength. The nanopore surface charge affects the translocation process through the EOF,²⁴ which arises from the electrostatic interaction between the electric field and mobile ions in the electric double layer (EDL).²⁹ For the applied electric field, as shown in Figure 1a, the EOF would always oppose the motion of the negatively charged molecules (e.g., DNAs) if the nanopore walls are negatively charged.³⁰ Another factor affecting the EOF is the ionic strength because the Debye length in the EDL is strongly salt concentration-dependent. It

has been previously observed in the experiment that DNA translocation in the glass nanopore is strongly salt-dependent.²³

To study the synergistic effect of both surface charge and ionic strength, we calculated the event rate of 100 pM DNA through a conical-shaped nanopore with a diameter of 12 nm and an angle of $\theta = 4^\circ$. Figure 2a plots the event rate heatmap, which clearly shows that the rate strongly depends on the ionic strength and surface charge density. We observed a few interesting features. First, for each specific ionic strength, the event rate reduces when the surface charge becomes more negative because of the increased retardation EOF. Figure 2b shows the event rate as a function of surface charge for various ionic strength conditions. The event rate was found to be exponentially increased when decreasing the surface charge. Second, at a specific surface charge density, working at higher ionic strength conditions would help to increase the event rate. This is because the EOF becomes less significant at higher salt concentrations. Figure 2c illustrates the event rate as a function of ionic strength for various surface charge conditions. The effect of ionic strength on the rate becomes less significant when the surface charge density reduces. For the case of zero surface charge, the ionic strength does not affect the event rate at all. Finally, Figure 2a also shows that working at low salt concentrations with a highly negatively charged nanopore would result in a very low event rate. The empty area in Figure 2a shows the region where the translation rate is less than 10^{-3} /s. This rate is impractical for gathering sufficient events

to build robust statistics within a reasonable amount of time. For instance, with a rate of 0.001 s^{-1} and an experiment time of 1 h, we can only expect to count less than four events.

These results have a few implications for the nanopore experiments. From the fast sensor response time perspective, working at higher ionic strengths with a nanopore of a lower surface charge would be favorable. Nevertheless, various bioassays have an upbound for the salt concentration.³¹ For example, the usual 1–4 M salt concentration used in a typical nanopore experiment might be detrimental for assays such as polymerase chain reaction and loop-mediated isothermal amplification.³² As a result, a neutral (or close to neutral) nanopore surface would be preferred for the experiments that require a specific salt condition.

Impact of the Nanopore Geometry. It was previously found that the electric field and EOF strongly depend on the nanopore geometry.³³ This suggests that alternation of the nanopore geometry is of potential use for enhancing the event rate. To this end, we examined the event rate of 100 pM DNA at an ionic strength of 1 M and a surface charge density of -20 mC/m^2 through nanopores of varying angles and diameters. Figure 3a illustrates the event rate heatmap, which clearly shows that the rate strongly depends on the nanopore diameters and angles.

Figure 3b shows the event rate as a function of nanopore diameters for four different angles. For a specific angle, the event rate increases linearly with the nanopore size. This is not surprising at first glance because a larger pore would be less resistive for the translocation. A detailed calculation reveals that the nanopore conductance is approximately linearly to r_p (Supporting Information Note S3). However, there is another factor that contributes to the enhanced rate. As the nanopore size increases, the effective electric field across the nanopore region would be reduced, which in turn reduces the opposing EOF flow. This result means a larger nanopore would be preferred from the response time perspective. However, the nanopore diameter needs to be comparable to the size of the analyte molecule to ensure single-molecule sensitivity and thus cannot be scaled up arbitrarily.

Figure 3c plots the event rate as a function of nanopore angles for four diameters. A clear enhancement of the rate was observed when increasing the nanopore angle (nanopore become more flattened). This effect was also because of the contributions of two factors. The first is the increase of the nanopore conductance (Supporting Information Note S3). The second is the reduced impact of EOF. To examine the impact of EOF, we calculated two representative cases: no surface charge (without EOF) and -20 mC/m^2 surface charge (with EOF). As shown in Figure 4a, the impact of nanopore angles on the rate is less significant for the case without the EOF. Moreover, the rates with the EOF are much less than that without the EOF, and the reduction is angle-dependent. As shown in Figure 4b, the EOF-induced rate reduction is much more significant at smaller angles.

Silicon Nitride Versus Glass Nanopores. The results shown in Figure 4 imply that a more widely opened nanopore would be preferred from the event rate perspective. For typical laser-pulled glass nanopores, the range of the angle is limited to be within $2\text{--}12^\circ$.^{34,35} On the other hand, membrane-based silicon nitride (SiN_x) nanopores represent another important nanopore geometry with an angle equal to 90° .³⁶ We set out to compare the event rate between the typical glass nanopore (Figure 5a) and SiN_x nanopores (Figure 5b). Both pores are

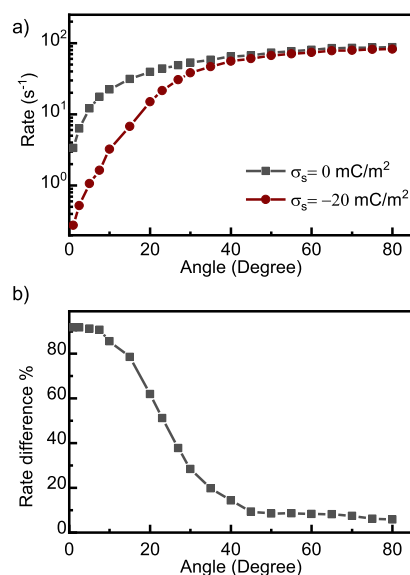


Figure 4. (a) 100 pM DNA event rate at different angles for a surface charge density of 0 (without EOF) and -20 mC/m^2 (with EOF), with a nanopore diameter of 12 nm and an ionic strength of 1 M, and (b) the rate difference percentage for different angles with and without EOF, defined as $(R_{\text{woEOF}} - R_{\text{wEOF}})/R_{\text{woEOF}}$.

assumed to have the same diameter of 12 nm. The glass nanopore is assumed to have an angle of $\theta = 4^\circ$. The heatmap in Figure 5a,b shows the event rate as a function of ionic strength and surface charge. To quantitatively evaluate the rate difference, Figure 5c plots the rate ratio between the SiN_x nanopore and the glass nanopore. It was found that the rate in the SiN_x nanopore is always higher than that in the glass nanopore under the same ionic strength and surface charge condition (note that an equal rate will have the log ratio of 0). This rate enhancement in the SiN_x nanopore is because of not only the less-resistive molecule transport path but also the less impact of the opposing EOF flow. The difference in the rate between the glass and SiN_x becomes more pronounced at low salt concentration and high surface charges, an expected feature that comes from the EOF dependence on the salt concentrations and surface charges. This result means that the membrane-based SiN_x nanopore is favorable to achieve a fast event rate as compared to the conical-shaped glass nanopore, giving everything else the same.

Impact of Direction. It was previously reported that DNA translocation in the glass nanopore is strongly salt- and direction-dependent,²³ consistent with our own observations (Figure S4). While broken symmetry induced asymmetric ionic transport behavior in nanofluidic diodes was well understood,³⁷ the impact of EOF on the transport process was neglected in most studies.³⁸ In addition, it was previously shown that EOF itself is asymmetric which can lead to the EOF rectification in conical nanopores.³⁹

Therefore, the electrophoretic flow and EOF should be considered together to understand the experimentally observed molecular rectification. To make the following discussion clear, we define the translocation out from and into the glass nanopore as forward and backward directions, respectively (Figure 6a,b). Note that this definition is opposite to that of Keyser et al.²³ Figure 6c,d plots the event rate under the influence of EOF as a function of ionic strength and surface charge for forward and backward configurations, respectively.

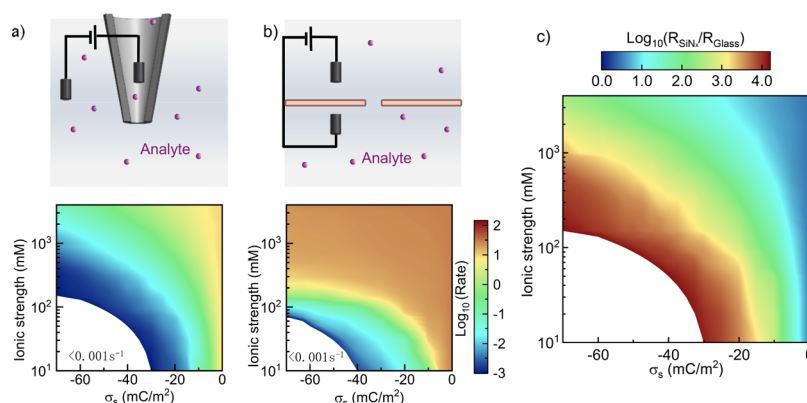


Figure 5. Event rate of 100 pM DNA through (a) conical-shaped glass nanopore, and (b) SiN_x nanopore, both with a diameter of 12 nm. (c) Translocation ratio between the SiN_x and glass nanopores as a function of surface charge density and the ionic strength.

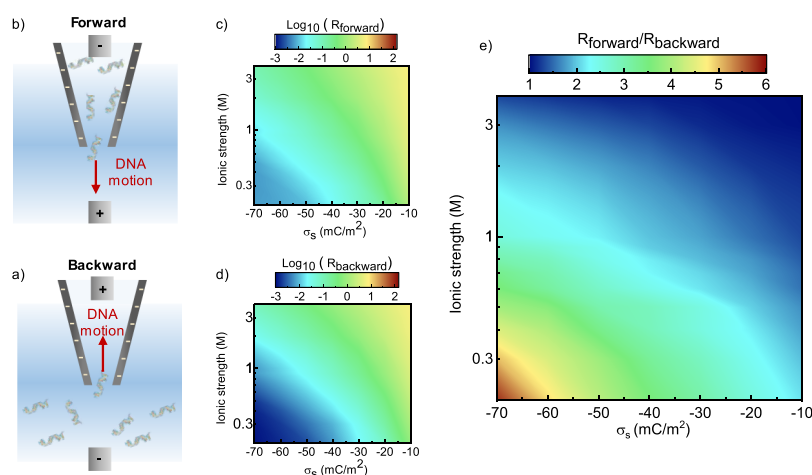


Figure 6. Schematic of DNA translocation in (a) forward and (b) backward direction, as well as the event rate of the 100 pM DNA through the 12 nm conical-shape nanopore in the (c) forward and (d) backward configurations. (e) Event rate ratio between the forward and backward configurations. The translocation rectification effect is more pronounced in the low salt and high surface charge region.

It is noteworthy that regardless of the translocation direction, EOF is always an opposing force against the DNA movement if the surface charge is negative, which means that the DNA event rate with EOF is always lower than that without the EOF. Figure 6e illustrates the ratio of $R_{\text{forward}}/R_{\text{backward}}$ (rate rectification ratio) at different surface charges and ionic strengths. It was clear that the rate in the forward direction is always larger than that in the reverse direction. In addition, the rate rectification ratio is more pronounced (ratio away from unity) when working at low ionic strengths with a highly charged nanopore surface because of the enhanced EOF rectification ratio in these regions.³⁹

These results elucidate the importance of EOF in molecule transport through the glass nanopore and provide experimental insights for enhancing the event rate. For example, if one can reverse the surface charge polarity through surface functionalization, the resulting EOF will always enhance the DNA event rate. In addition, loading the analyte molecules into the glass nanopore for analysis would be preferred from the rate enhancement perspective.

CONCLUSIONS

In summary, we presented a comprehensive study of factors affecting the event rate in glass nanopore sensors. This event rate-focused study aims to provide useful and practical insight

to enhance the device response time for various glass nanopore-sensing experiments. We found that while the event rate intrinsically depends on the analyte concentration and mobility (linearly), factors such as nanopore surface charge density, geometry, ionic strength, and the translocation direction could impact the event rate nonlinearly by orders of magnitude. From the standpoint of enhancing the response time in glass nanopore sensors, higher ionic strength, lower nanopore surface charge (neutral surface is ideal), and less vertical nanopore walls would be desirable because of the reduced impact of the opposing EOF. Because of the negative surface charge in glass nanopores, translocation from the glass nanopore could be orders of magnitude faster than that into the nanopore at low salt concentrations and higher surface charges. Therefore, attention should be paid when setting up the translocation direction in the glass nanopore because of the EOF rectification. In addition, we found that SiN_x membrane-based nanopores are generally favorable over glass nanopores for achieving a fast response, especially when working with low ionic strength and higher surface charge densities. We anticipate that these findings would provide insight for future glass nanopore-sensing experiments toward ultrasensitive sensing applications where the device response time is of significant importance.

■ ASSOCIATED CONTENT

■ Supporting Information

The Supporting Information is available free of charge on the ACS Publications website at DOI: [10.1021/acssensors.9b01540](https://doi.org/10.1021/acssensors.9b01540).

Detailed descriptions of the computational domain, boundary conditions, and parameters, event rate as a function of electrophoretic mobility, translocation recording of λ -DNA through the glass nanopore for backward and forward configurations, the dominance of diffusion-limited transport in most glass nanopores, average molecular distance estimation, and glass nanopore conductance derivation (PDF)

■ AUTHOR INFORMATION

Corresponding Author

*E-mail: w.guan@psu.edu. Phone: 1-814-867-5748.

ORCID

Weihua Guan: [0000-0002-8435-9672](https://orcid.org/0000-0002-8435-9672)

Notes

The authors declare no competing financial interest.

■ ACKNOWLEDGMENTS

This work is supported by the National Science Foundation under grant nos. 1710831, 1902503, and 1912410. Any opinions, findings, and conclusions or recommendations expressed in this work are those of the authors and do not necessarily reflect the views of the National Science Foundation. W.G. acknowledges support from Penn State Startup Fund.

■ REFERENCES

- (1) Firnkes, M.; Pedone, D.; Knezevic, J.; Döblinger, M.; Rant, U. Electrically facilitated translocations of proteins through silicon nitride nanopores: conjoint and competitive action of diffusion, electrophoresis, and electroosmosis. *Nano Lett.* **2010**, *10*, 2162–2167.
- (2) Li, J.; Gershow, M.; Stein, D.; Brandin, E.; Golovchenko, J. A. DNA molecules and configurations in a solid-state nanopore microscope. *Nat. Mater.* **2003**, *2*, 611–615.
- (3) Smeets, R. M. M.; Kowalczyk, S. W.; Hall, A.; Dekker, N.; Dekker, C. Translocation of RecA-coated double-stranded DNA through solid-state nanopores. *Nano Lett.* **2009**, *9*, 3089–3095.
- (4) Steinbock, L. J.; Bulushev, R. D.; Krishnan, S.; Raillon, C.; Radenovic, A. DNA translocation through low-noise glass nanopores. *ACS Nano* **2013**, *7*, 11255–11262.
- (5) Lan, W.-J.; Holden, D. A.; Zhang, B.; White, H. S. Nanoparticle transport in conical-shaped nanopores. *Anal. Chem.* **2011**, *83*, 3840–3847.
- (6) Bell, N. A. W.; Muthukumar, M.; Keyser, U. F. Translocation frequency of double-stranded DNA through a solid-state nanopore. *Phys. Rev. E* **2016**, *93*, 022401.
- (7) Garaj, S.; Hubbard, W.; Reina, A.; Kong, J.; Branton, D.; Golovchenko, J. A. Graphene as a subnanometre trans-electrode membrane. *Nature* **2010**, *467*, 190–193.
- (8) Miles, B. N.; Ivanov, A. P.; Wilson, K. A.; Doğan, F.; Japrun, D.; Edel, J. B. Single molecule sensing with solid-state nanopores: novel materials, methods, and applications. *Chem. Soc. Rev.* **2013**, *42*, 15–28.
- (9) Rosen, C. B.; Rodriguez-Larrea, D.; Bayley, H. Single-molecule site-specific detection of protein phosphorylation with a nanopore. *Nat. Biotechnol.* **2014**, *32*, 179–181.
- (10) Japrun, D.; Dogan, J.; Freedman, K. J.; Nadzeyka, A.; Bauerdick, S.; Albrecht, T.; Kim, M. J.; Jemth, P.; Edel, J. B. Single-

molecule studies of intrinsically disordered proteins using solid-state nanopores. *Anal. Chem.* **2013**, *85*, 2449–2456.

(11) Shasha, C.; Henley, R. Y.; Stoffer, D. H.; Rynearson, K. D.; Hermann, T.; Wanunu, M. Nanopore-based conformational analysis of a viral RNA drug target. *ACS Nano* **2014**, *8*, 6425–6430.

(12) Zhang, M.; Yeh, L.-H.; Qian, S.; Hsu, J.-P.; Joo, S. W. DNA Electrokinetic translocation through a nanopore: local permittivity environment effect. *J. Phys. Chem. C* **2012**, *116*, 4793–4801.

(13) Albrecht, T. Single-Molecule Analysis with Solid-State Nanopores. *Annu. Rev. Anal. Chem.* **2019**, *12*, 371–387.

(14) Wanunu, M.; Morrison, W.; Rabin, Y.; Grosberg, A. Y.; Meller, A. Electrostatic focusing of unlabelled DNA into nanoscale pores using a salt gradient. *Nat. Nanotechnol.* **2010**, *5*, 160–165.

(15) Nouri, R.; Tang, Z.; Guan, W. Calibration-Free Nanopore Digital Counting of Single Molecules. *Anal. Chem.* **2019**, *91*, 11178–11184.

(16) Wu, Y.; Tilley, R. D.; Gooding, J. J. Challenges and Solutions in Developing Ultrasensitive Biosensors. *J. Am. Chem. Soc.* **2018**, *141*, 1162–1170.

(17) Squires, T. M.; Messinger, R. J.; Manalis, S. R. Making it stick: convection, reaction and diffusion in surface-based biosensors. *Nat. Biotechnol.* **2008**, *26*, 417–426.

(18) Freedman, K. J.; Otto, L. M.; Ivanov, A. P.; Barik, A.; Oh, S.-H.; Edel, J. B. Nanopore sensing at ultra-low concentrations using single-molecule dielectrophoretic trapping. *Nat. Commun.* **2016**, *7*, 10217.

(19) Gooding, J. J.; Gaus, K. Single-Molecule Sensors: Challenges and Opportunities for Quantitative Analysis. *Angew. Chem., Int. Ed.* **2016**, *55*, 11354–11366.

(20) Kelley, S. O.; Mirkin, C. A.; Walt, D. R.; Ismagilov, R. F.; Toner, M.; Sargent, E. H. Advancing the speed, sensitivity and accuracy of biomolecular detection using multi-length-scale engineering. *Nat. Nanotechnol.* **2014**, *9*, 969–980.

(21) Hatlo, M. M.; Panja, D.; van Rooij, R. Translocation of DNA molecules through nanopores with salt gradients: the role of osmotic flow. *Phys. Rev. Lett.* **2011**, *107*, 068101.

(22) Grosberg, A. Y.; Rabin, Y. DNA capture into a nanopore: interplay of diffusion and electrohydrodynamics. *J. Chem. Phys.* **2010**, *133*, 165102.

(23) Chen, K.; Bell, N. A. W.; Kong, J.; Tian, Y.; Keyser, U. F. Direction- and salt-dependent ionic current signatures for DNA sensing with asymmetric nanopores. *Biophys. J.* **2017**, *112*, 674–682.

(24) He, Y.; Tsutsui, M.; Fan, C.; Taniguchi, M.; Kawai, T. Controlling DNA translocation through gate modulation of nanopore wall surface charges. *ACS Nano* **2011**, *5*, 5509–5518.

(25) Crick, C. R.; Albella, P.; Ng, B.; Ivanov, A. P.; Roschuk, T.; Cecchini, M. P.; Bresme, F.; Maier, S. A.; Edel, J. B. Precise attoliter temperature control of nanopore sensors using a nanoplasmonic bullseye. *Nano Lett.* **2014**, *15*, 553–559.

(26) Nicoli, F.; Verschuere, D.; Klein, M.; Dekker, C.; Jonsson, M. P. DNA translocations through solid-state plasmonic nanopores. *Nano Lett.* **2014**, *14*, 6917–6925.

(27) Ivanov, A. P.; Actis, P.; Jönsson, P.; Klennerman, D.; Korchev, Y.; Edel, J. B. On-demand delivery of single DNA molecules using nanopipets. *ACS Nano* **2015**, *9*, 3587–3595.

(28) Stellwagen, N. C.; Gelfi, C.; Righetti, P. G. The free solution mobility of DNA. *Biopolymers* **1997**, *42*, 687–703.

(29) Kirby, B. J.; Hasselbrink, E. F., Jr. Zeta potential of microfluidic substrates: 1. Theory, experimental techniques, and effects on separations. *Electrophoresis* **2004**, *25*, 187–202.

(30) Lin, D.-H.; Lin, C.-Y.; Tseng, S.; Hsu, J.-P. Influence of electroosmotic flow on the ionic current rectification in a pH-regulated, conical nanopore. *Nanoscale* **2015**, *7*, 14023–14031.

(31) Yang, W.; Restrepo-Pérez, L.; Bengtson, M.; Heerema, S. J.; Birnie, A.; van der Torre, J.; Dekker, C. Detection of CRISPR-dCas9 on DNA with Solid-State Nanopores. *Nano Lett.* **2018**, *18*, 6469–6474.

(32) Zhou, D.; Guo, J.; Xu, L.; Gao, S.; Lin, Q.; Wu, Q.; Wu, L.; Que, Y. Establishment and application of a loop-mediated isothermal

amplification (LAMP) system for detection of cry1Ac transgenic sugarcane. *Sci. Rep.* **2014**, *4*, 4912.

(33) Timp, W.; Mirsaidov, U. M.; Wang, D.; Comer, J.; Aksimentiev, A.; Timp, G. Nanopore sequencing: electrical measurements of the code of life. *IEEE Trans. Nanotechnol.* **2010**, *9*, 281–294.

(34) Lan, W.-J.; Holden, D. A.; Liu, J.; White, H. S. Pressure-driven nanoparticle transport across glass membranes containing a conical-shaped nanopore. *J. Phys. Chem. C* **2011**, *115*, 18445–18452.

(35) Tseng, S.; Lin, S.-C.; Lin, C.-Y.; Hsu, J.-P. Influences of cone angle and surface charge density on the ion current rectification behavior of a conical nanopore. *J. Phys. Chem. C* **2016**, *120*, 25620–25627.

(36) Roshan, K. A.; Tang, Z.; Guan, W. High fidelity moving Z-score based controlled breakdown fabrication of solid-state nanopore. *Nanotechnology* **2019**, *30*, 095502.

(37) Guan, W.; Fan, R.; Reed, M. A. Field-effect reconfigurable nanofluidic ionic diodes. *Nat. Commun.* **2011**, *2*, 506.

(38) White, H. S.; Bund, A. Ion current rectification at nanopores in glass membranes. *Langmuir* **2008**, *24*, 2212–2218.

(39) Laohakunakorn, N.; Keyser, U. F. Electroosmotic flow rectification in conical nanopores. *Nanotechnology* **2015**, *26*, 275202.